

Synthesis of ZnO nanoparticles through the impregnated layer combustion synthesis process

F. A. Deorsola · D. Vallauri

Received: 31 March 2010/Accepted: 30 July 2010/Published online: 17 August 2010
© Springer Science+Business Media, LLC 2010

Abstract Zinc oxide nanopowders were synthesized by a solution combustion technique named impregnated layer combustion synthesis (ILCS), involving the impregnation of an active layer with the reactant solution and subsequently the combustion of the impregnated system. In this work three different organic fuels and two different ignition modes were tested in order to optimize the final microstructure and specific surface area (SSA) of the ZnO nanopowders. In particular, the ignition mode was found to significantly affect the final products, discriminating between an explosion procedure (flame combustion) and a self-propagating mode (smoldering combustion). The nitrate–glycine mixture and the smoldering combustion way were found to be the most suitable conditions, giving rise to softly agglomerated nanopowders with an average size of 20 nm and a very high SSA, without the need of any further crystallization treatment.

Introduction

Zinc oxide (ZnO) is a very promising n-type semiconductor, with a wide band gap (3.37 eV) and a large exciton binding energy (60 meV). It has recently received growing interest due to its multifunctional and attractive properties, such as the photocatalytic behaviour. ZnO has been considered for a wide range of applications, such as ceramic electronic devices [1], chemical sensors [2–4], microwave absorption [5, 6] and wastewater treatment [7, 8]. In particular, the

attention has been focused on the photoelectric applications, like for instance UV-light emitters [9, 10], photocatalysis [11], window for display and solar cells for low-cost photovoltaic devices [12–14]. The possibility of introducing the nanoscale opens new interesting chemical and physical properties compared to microstructured zinc oxide, in terms of enhanced sinterability, improved photocatalytic behaviour, surface properties, etc. A significant variety of innovative technologies and processes have been developed in the last years for the synthesis of zinc oxide nanopowders, such as hydrothermal and solvothermal synthesis [15, 16], sol–gel [17, 18], spray pyrolysis [19, 20], mechanochemical processing [21], combustion oxidation [22, 23] and solution combustion synthesis [24, 25].

The solution combustion syntheses (SCS) represent an innovative and attractive approach for the production of a wide variety of tailored oxide nanoparticles. The process combines the combustion-based techniques, well-known in the literature as self-propagating high temperature synthesis (SHS), and the use of reactive solutions. It involves an exothermic redox reaction in solutions containing an oxidizer (metal nitrate) and a fuel compound. In the typical practice, after an initial heating the reaction ignites and self-sustains over the whole volume (known as volume combustion synthesis—VCS mode). The main advantages of the method are: (i) the mixture of reactants in the liquid state allows to obtain accurate compositions and constituent phases mixed at molecular level; (ii) the high temperatures of reaction assure high-purity and well-crystallized final powders; (iii) the very short reaction time and the significant development of gases hinder the particle grain growth and favour the formation of nanoparticles with high specific surface area (SSA) [26].

The basic VCS mode can be considered a very close approach to thermal explosion, with its characteristic

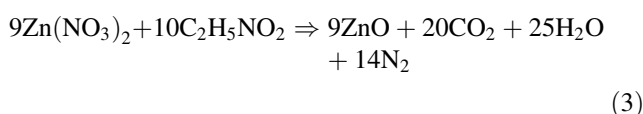
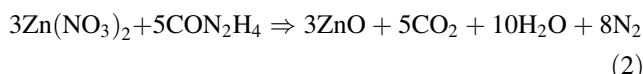
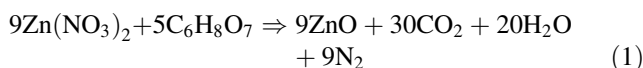
F. A. Deorsola (✉) · D. Vallauri
Dipartimento di Scienza dei Materiali e Ingegneria Chimica,
Politecnico di Torino, Corso Duca degli Abruzzi 24,
10129 Torino, Italy
e-mail: fabio.deorsola@polito.it

drawbacks related to the poor control of the process and to the low product yield. For this reason, it would be preferable to perform the reaction in a steady-state mode, more similar to that employed in the SHS. A novel technique, called impregnated active layer combustion (IALC) or impregnated layer combustion synthesis (ILCS) has been recently developed by Mukasyan et al. [26–28]. It is based on the impregnation of the reactive solution into a porous media that also participates to the reaction and favours the propagation of the reaction. The active layer has to satisfy some requirements, mainly its reaction products have to be in the gaseous phase so as to do not interfere with the final composition, and its process parameters must involve low temperatures and short times so as to facilitate the achievement of nanoparticles. These characteristics suggest the use of a thin layer of cellulose paper as active layer. The IALC approach, besides ensuring the steady-state propagation mode and thus a stricter control of the reaction for obtaining nanoparticles, allows to easily and efficiently plan the process in a continuous way. This represents an attractive perspective for a possible scale up of the combustion synthesis to the industrial level.

In this work, the IALC method has been employed for the synthesis of ZnO nanopowders. The effect of the process parameters on the final morphological properties of the nanopowders has been investigated. In particular, the kind of organic fuel and the mode of ignition have been studied. The optimized conditions allowed to obtain ZnO nanopowders with particle size of 20 nm and high SSA.

Experimental procedure

Zinc nitrate hexahydrate $\text{Zn}(\text{NO}_3)_2 \cdot 6\text{H}_2\text{O}$ was employed as metal precursor. Three different organic fuels were employed: citric acid $\text{C}_6\text{H}_8\text{O}_7 \cdot \text{H}_2\text{O}$, urea CON_2H_4 and glycine $\text{C}_2\text{H}_5\text{NO}_2$. All reactants were supplied by Sigma-Aldrich. The metal salt was dissolved into distilled water with a proper content of one combustible so as to perform reactions in stoichiometric conditions, according to the following redox reactions:



The molar concentration of the zinc nitrate in the aqueous solution was fixed to 1. After the reactants were

completely dissolved, a proper number of ashless paper sheets were impregnated with the solution and then dried at 40 °C for 12 h. The dried paper layers were ignited by putting them in a furnace kept at a constant temperature of 500 °C in static air. The thermal treatment took 30 min for the completion of the reaction and a sufficient crystallization of the nanopowders. In an alternative configuration, the dried paper layers were ignited in a suitable reaction chamber with dynamic air by a graphite rod heated by Joule effect. In this case, after ignition the energy supply was interrupted and the reaction self-sustained through the whole layers. A schematic view of the reactor set is illustrated in Fig. 1. The two ignition mode will be identified afterwards as “furnace combustion” and “reactor combustion”, respectively.

The study of the three different organic fuels was carried out by performing reactions in the “furnace combustion” mode. The combustible giving the most interesting results in terms of microstructure was further investigated in the “reactor combustion” mode for evaluating the influence of the ignition conditions on the final properties of the nanopowders.

For the sake of clarity, the nanopowders obtained in the “furnace combustion” mode by using citric acid, urea and glycine, respectively, will be named hereafter S1, S2 and S3, whereas the nanoparticles obtained in the “reaction combustion” mode by employing glycine will be identified as S4.

The produced nanopowders and the relative process conditions are summarized in Table 1. The syntheses were repeated three times for each process condition in order to verify the reproducibility.

The synthesized nanoparticles were characterized by X-ray diffraction (X’Pert Philips, range 2θ : 10°–70°, radiation $\text{Cu K}\alpha$, $\lambda = 1.54056 \text{ \AA}$), thermogravimetric analysis (Mettler Toledo, 50/1000 °C, 10 °C/min, air),

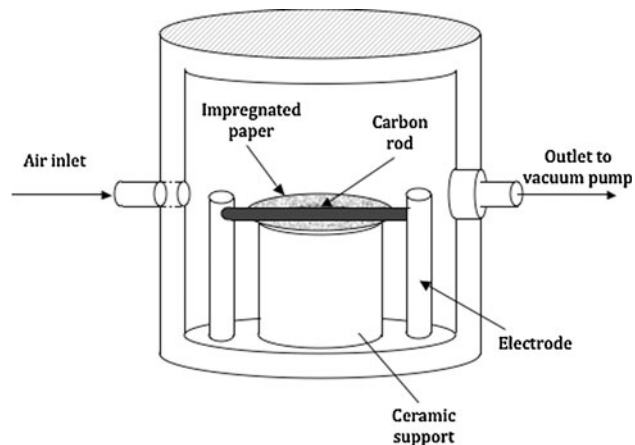


Fig. 1 Schematic view of the reaction set employed in the “reactor combustion” mode

Table 1 Process conditions, mean particle size calculated from the FESEM or TEM micrographs and specific surface area of the ZnO nanopowders produced by IALC

Sample name	Organic fuel	Ignition mode	Mean particle size (nm)	Specific surface Area (m^2/g)
S1	Citric acid	Furnace	30	16
S2	Urea	Furnace	55	17
S3	Glycine	Furnace	33	24
S4	Glycine	Reactor	20	71

BET SSA by means of nitrogen adsorption–desorption at 77 K (Micromeritics ASAP 2010), field emission scanning electron microscopy (Leo Supra 40) and transmission electron microscopy (Hitachi H-7100).

Results and discussion

The XRD patterns of the nanopowders obtained by varying the kind of organic fuel and the ignition mode are illustrated in Fig. 2. For all samples, the characteristic peaks at 31.77, 34.42 and 36.25 two-theta degree was recognized, corresponding to the $h\bar{k}\bar{l}$ Miller index (100), (002) and (101), respectively [29]. The nanopowders showed a sufficient degree of crystallization, allowing to avoid a subsequent calcination treatment at high temperature.

Thermogravimetric analysis on the dried paper impregnated with the solutions containing the three different fuels was carried out, as reported in Fig. 3. As can be noticed, the behaviour of the impregnated paper was significantly different depending on the kind of fuel employed. Starting from the sequence reported in the literature [30], the paper alone shows two stages during the thermal decomposition in

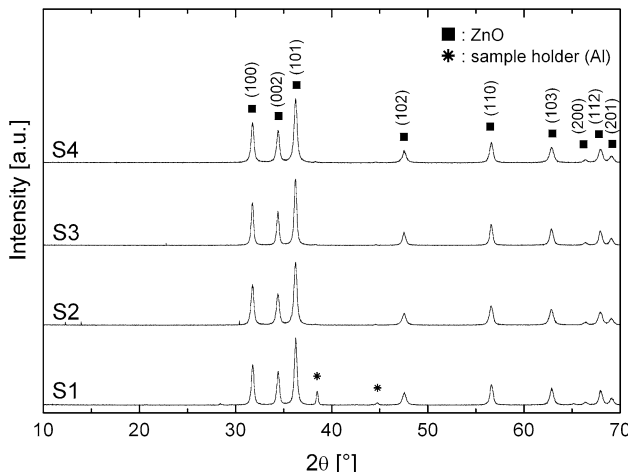


Fig. 2 XRD patterns of the as-synthesized ZnO nanopowders obtained by IALC

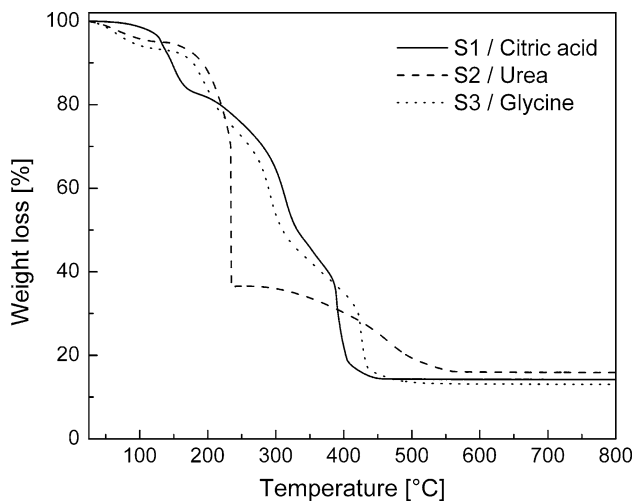


Fig. 3 TGA curves of the paper impregnated with solution containing citric acid (solid), urea (dash) and glycine (dot) in the synthesis of ZnO nanopowders by means of IALC

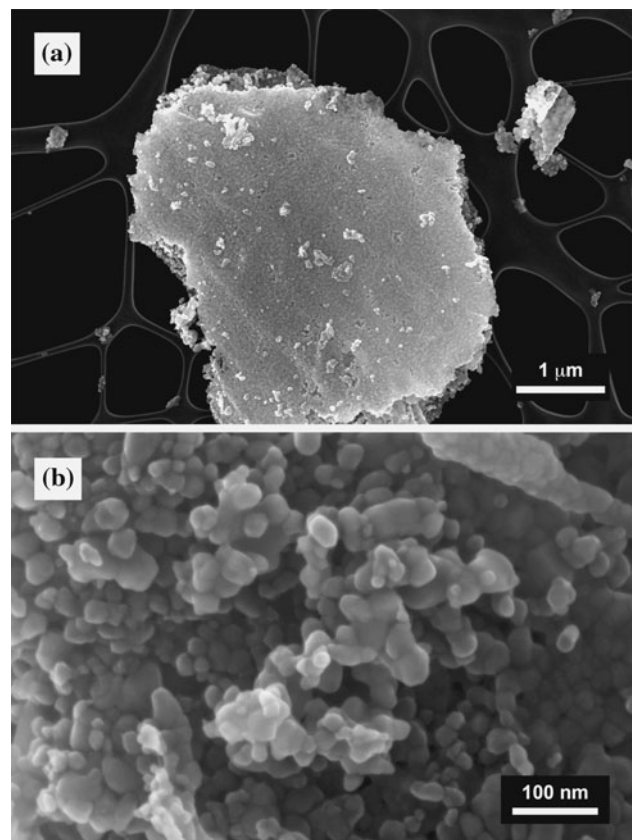


Fig. 4 FESEM micrographs of the S1 nanopowders synthesized by employing citric acid as organic fuel and the “furnace combustion” mode

air, corresponding to the depolymerisation of the cellulose chains and their oxidative degradation and to the pyrolysis of the carbonaceous char. The total pyrolysis is completed before 500 °C.

The papers impregnated with solution containing citric acid and glycine showed a similar behaviour, in which the reactants decomposed and the redox reaction occurred (in the range between 100 and 300 °C), supplying sufficient heat to complete the degradation of the paper (at 400–440 °C depending on the fuel). The residual product is constituted by only ZnO and its content is 13 wt% with respect to the starting mass by employing glycine and 14% by using citric acid. On the contrary, in the case of urea the reaction occurred at 250 °C characterized by a nearly explosive behaviour, due to the presence of two amine groups in the fuel molecule. The extreme exothermicity allowed to simultaneously carry out the degradation of paper, and the subsequent weight loss is due to the pyrolysis of carbonaceous residues. The final residue of ZnO was valued as 15%, with a final yield quite similar to the other combustibles.

From the thermal analysis, some advantages can be drawn for IALC in comparison to the traditional solution combustion and gel combustion. Generally, the SCS process is characterized by very exothermic reactions, meaning explosive behaviour more or less pronounced depending on the organic fuel employed [31, 32]. In the

case of ZnO synthesis, the use of paper leads to a similar trend in terms of progress of the reaction, but is significantly more effective than the other combustion techniques by acting as support for a more uniform heat transfer and propagation of the reaction, by increasing the development of gases inhibiting the particle growth and by supplying some additional heating for the instantaneous crystallization of the nanopowders.

Some significant differences between the nanopowders synthesized by varying the process parameters as indicated above were revealed by the FESEM analysis. The micrographs for sample S1, reported in Fig. 4, showed the presence of nanoparticles strongly agglomerated. The agglomerates were characterized by micrometric dimensions (Fig. 4a) whereas the nanoparticles were sized in the range between 10 and 30 nm, with spherical and reproducible shape.

It is worth to mention that the nanopowders agglomerates traced faithfully the structure of the paper cellulose used as active layer and actively participating to the redox reaction, as showed in Fig. 5a for sample S2. However, also in this case the nanopowders resulted strongly agglomerated and their dimensions were slightly higher

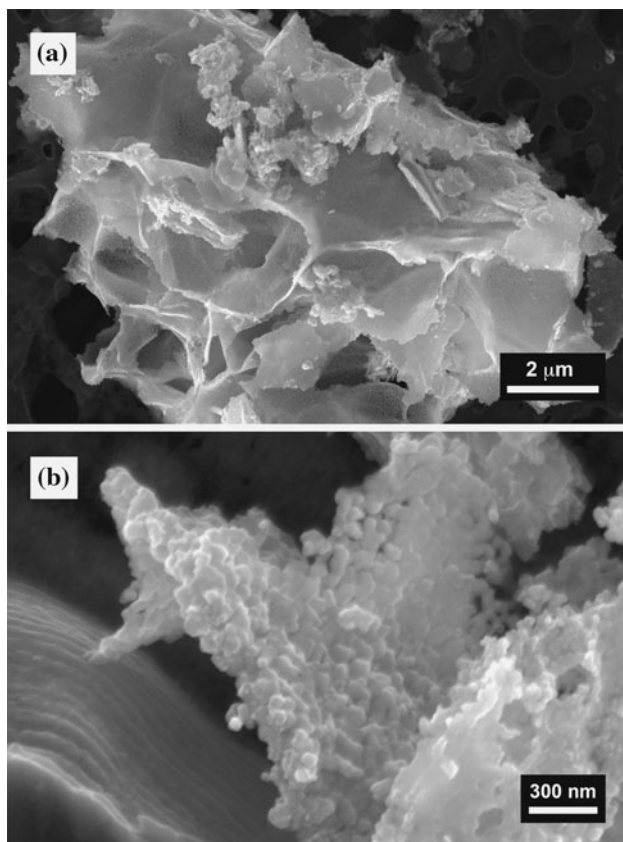


Fig. 5 FESEM micrographs of the S2 nanopowders synthesized by employing urea as organic fuel and the “furnace combustion” mode

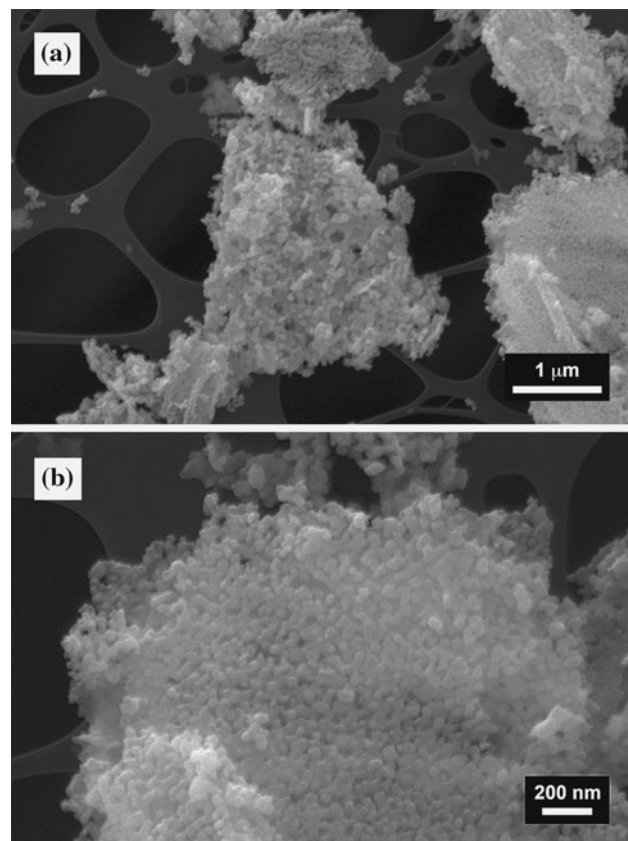


Fig. 6 FESEM micrographs of the S3 nanopowders synthesized by employing glycine as organic fuel and the “furnace combustion” mode

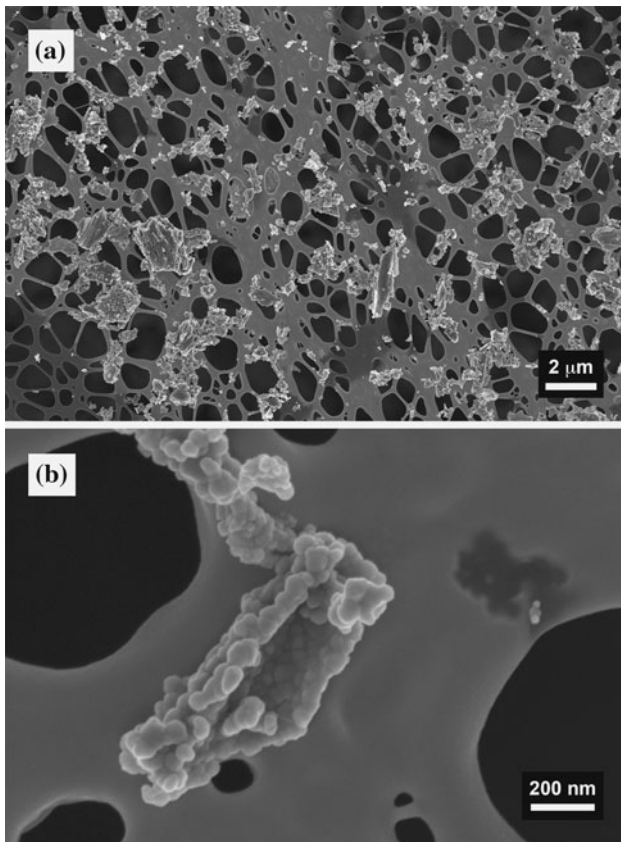


Fig. 7 FESEM micrographs of the S4 nanopowders synthesized by employing glycine as organic fuel and the “reactor combustion” mode

than those of the S1 ones (Fig. 5b). It follows that, for the system ZnO and for the syntheses performed in the described conditions (furnace ignition), the mixtures nitrate–citric acid and nitrate–urea showed a very similar behaviour in terms of exothermicity, reaction velocity and development of gases, yielding to a marked similarity in the morphology of the nanopowders.

On the other hand, the synthesis performed by using glycine and ignited in the furnace mode gave some different results in the microstructure of the nanopowders. As can be noticed in Fig. 6, the agglomerates maintained the micrometric size (Fig. 6a), but nanopowders showed a lower degree of agglomeration and the distribution of the particles size was narrower and more uniform (Fig. 6b). The better behaviour of the reaction with glycine was confirmed by the specific surface characterization, with a SSA value of $24 \text{ m}^2/\text{g}$ compared to 16 and $17 \text{ m}^2/\text{g}$ of the samples S1 and S2, respectively. The low values of the SSA, considered in absolute terms, confirmed the high level of agglomeration of these nanopowders, as shown by the FESEM micrographs reported in Figs. 4, 5 and 6.

Since the employment of glycine gave the best results in terms of microstructure and SSA, the mixture

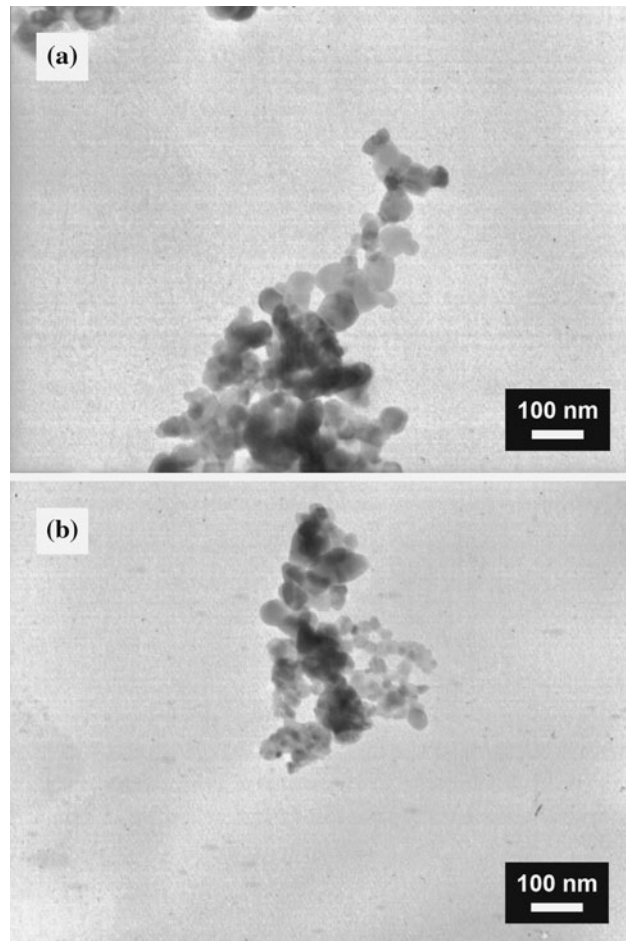


Fig. 8 TEM micrographs of **a** S3 nanopowders synthesized by employing glycine as organic fuel and the “furnace combustion” mode and **b** S4 nanopowders synthesized by employing glycine as organic fuel and the “reactor combustion” mode

nitrate–glycine was tested by using the “reactor ignition” mode. Whereas in the “furnace mode” the reaction proceeded in a very rapid way, with the development of flame, in this case the combustion waves propagated in a smouldering way, significantly affecting the final properties of the nanopowders. In fact, as reported in Fig. 7, the dimension of agglomerates was decreased to some hundreds of nanometres (Fig. 7a). The nanopowders showed uniform dimension of about 20 nm (Fig. 7b) and the SSA was significantly increased, with a value of $71 \text{ m}^2/\text{g}$. The SSA values obtained and the mean particles sizes calculated from the micrographs are summarized for comparison in Table 1.

The difference between the two ignition modes can be further appreciated in the TEM micrographs, illustrated in Fig. 8. By the steady-state propagation (Fig. 8b) it was possible to decrease the agglomerate dimension and especially to lower the grain size. As previously demonstrated by Mukasyan and Dinka [26] in the production of other

nanometric oxides, the smoldering propagation mode, realized in this work by the “reactor mode” ignition, seems to be a more effective synthesis way yielding soft agglomerates of nanopowders with very high SSA values.

Conclusions

Zinc oxide nanopowders were successfully synthesized by an ILCS method. The ILCS technique was demonstrated to be effective in the production of ZnO nanopowders, especially in the perspective of a continuous apparatus for large-scale runs. The kind of organic fuel and the ignition mode were tested as process parameters. All samples showed the reaction completion and the formation of well-crystallized nanopowders. The fuel quality was found to slightly affect the powder characteristics in terms of size, morphology and SSA, with the best results given by the mixture nitrate–glycine. On the other hand, the effect of the ignition mode was proved to be significative. In fact, a smoldering combustion type instead of a rapid flame one allowed to decrease the agglomeration degree and the agglomerate size and to obtain very uniform nanopowders with average grain size of 20 nm and SSA of 71 m²/g.

Acknowledgement The authors gratefully acknowledge Professor I. Amato for the overview of the technical work and the useful discussion.

References

1. Singhal M, Chhabra V, Kang P, Shah DO (1997) Mater Res Bull 32:239
2. de Lacy Costello BPJ, Ewen RJ, Guernion N, Ratcliffe NM (2002) Sens Actuators B 87:207
3. Yamazoe N, Sakai G, Shimanoe K (2003) Catal Surv Asia 7:63
4. Baruwati B, Kumar DK, Manorama SV (2006) Sens Actuators B 119:676
5. Cao MS, Shi XL, Fang XY, Jin HB, Hou ZL, Zhou W, Chen YJ (2007) Appl Phys Lett 91:203110
6. Shi XL, Yuan J, Zhou W, Rong JL, Cao MS (2007) Chin Phys Lett 24:2994
7. Park S, Lee JC, Kim BS, Lee JH (2005) J Mater Sci 40:5327. doi:[10.1007/s10853-005-4399-9](https://doi.org/10.1007/s10853-005-4399-9)
8. Park S, Lee JH, Kim HS, Park HJ, Lee JC (2009) J Electroceram 22:105
9. Zhao YN, Cao MS, Li JG, Chen YJ (2006) J Mater Sci 41:2243. doi:[10.1007/s10853-006-7176-5](https://doi.org/10.1007/s10853-006-7176-5)
10. Zhao YN, Cao MS, Jin HB, Zhang L, Qiu CJ (2006) Scr Mater 54:2057
11. Shaporev AS, Ivanov VK, Baranchiko AE, Tret'yakov YD (2007) Inorg Mater 43:35
12. Look DC (2001) Mater Sci Eng B 80:383
13. Pearton SJ, Norto DP, Ip K, Heo YW, Steiner T (2005) Prog Mater Sci 50:293
14. Sheng X, Zhao Y, Zhai J, Jiang L, Zhu D (2007) Appl Phys A 87:715
15. Cai KF, He XR, Zhang LC (2008) Mater Lett 62:1223
16. Moghaddam FM, Saeidian H (2007) Mater Sci Eng B 139:265
17. El Mir L, El Ghoul J, Alaya S, Ben Salem M, Barthou C, von Bardeleben HJ (2008) Physica B 403:1770
18. Mondelaers D, Vanhooyland G, Van den Rul H, Haen JD, Van Bael MK, Mullens J, Van Poucke LC (2002) Mater Res Bull 37:901
19. Tani T, Watanabe N, Takatori K (2003) J Nanopart Res 5:39
20. Singh P, Kumar A, Deepak, Kaur D (2007) J Cryst Growth 306:303
21. Dodd A, McKinley A, Tsuzuki T, Saunders M (2008) J Nanopart Res 10:243
22. Zhao YN, Cao MS, Li JG, Chen YJ (2005) Mater Res Bull 40:1745
23. Shi XL, Cao MS, Zhao YN, Song WL, Rong JL (2008) Sci China Ser E 51:1433
24. Park S, Lee JC, Lee DW, Lee JH (2003) J Mater Sci 38:4493. doi:[10.1023/A:1027329501367](https://doi.org/10.1023/A:1027329501367)
25. Lin CS, Hwang CC, Lee WH, Tong WY (2007) Mater Sci Eng B 140:31
26. Mukasyan AS, Dinka P (2007) Int J SHS 16:23
27. Mukasyan AS, Dinka P (2007) Adv Eng Mater 9:653
28. Kumar A, Mukasyan AS, Wolf EE (2010) Appl Catal A 372:175
29. ZnO JCPDS card for X-ray pattern (JCPDS 36-1451)
30. Kashiwagi T, Nambu H (1992) Combust Flame 88:345
31. Hwang CC, Wu TY (2004) Mater Sci Eng B 111:197
32. Hwang CC, Wu TY (2004) J Mater Sci 39:6111. doi:[10.1023/B:JMSC.0000041713.37366.c2](https://doi.org/10.1023/B:JMSC.0000041713.37366.c2)